OAK RIDGE NATIONAL LABORATORY LIBRARIES
3 4456 0550240 8

CENTRAL RESEARCH LIBRARY
ORNL-TM-4535

Cy 26

ISOTOPIC POWER MATERIALS DEVELOPMENT PROGRESS REPORT FOR JANUARY 1974

R. G. Donnelly

[redacted]

OAK RIDGE NATIONAL LABORATORY
CENTRAL RESEARCH LIBRARY
DOCUMENT COLLECTION
LIBRARY LOAN COPY
DO NOT TRANSFER TO ANOTHER PERSON
If you wish someone else to see this document, send in name with document and the library will arrange a loan.
UCN-7969
(3 3-67)

OAK RIDGE NATIONAL LABORATORY
OPERATED BY UNION CARBIDE CORPORATION • FOR THE U.S. ATOMIC ENERGY COMMISSION

This report was prepared as an account of work sponsored by the United States Government. Neither the United States nor the United States Atomic Energy Commission, nor any of their employees, nor any of their contractors, subcontractors, or their employees, makes any warranty, express or implied, or assumes any legal liability or responsibility for the accuracy, completeness or usefulness of any information, apparatus, product or process disclosed, or represents that its use would not infringe privately owned rights.

ORNL-TM-4535

Contract No. W-7405-eng-26

METALS AND CERAMICS DIVISION

ISOTOPIC POWER MATERIALS DEVELOPMENT PROGRESS REPORT FOR JANUARY 1974

R. G. Donnelly

MAY 1974

NOTICE This document contains information of a preliminary nature and was prepared primarily for internal use at the Oak Ridge National Laboratory. It is subject to revision or correction and therefore does not represent a final report.

OAK RIDGE NATIONAL LABORATORY
Oak Ridge, Tennessee 37830
operated by
UNION CARBIDE CORPORATION
for the
U.S. ATOMIC ENERGY COMMISSION

OAK RIDGE NATIONAL LABORATORY LIBRARIES

3 4456 0550240 8

CONTENTS

Page

IRIDIUM FABRICATION PROGRAM 1
Fabrication of Iridium for PICS 1
Cleaning Ir–0.3% W Sheet 1
Recrystallization of Ir–0.3% W Sheet 3
Rolling 0.005-in. Thick Ir–0.3% W Sheet 5
HIGH-TEMPERATURE ALLOYS FOR SPACE ISOTOPIC HEAT SOURCES 7
Development of Iridium Alloys 7
Tensile Properties 7
Air Oxidation 7
Scaleup of Iridium-Base Alloys 7
Postmortem of MHT-74 10
Ruthenium Characterization and Fabrication Development 11
Platinum-Rhodium-Tungsten Alloys 11
Fabrication Development 11
Fabrication of Compatibility Components 12
PHYSICAL AND MECHANICAL METALLURGY OF HEAT SOURCE CONTAINMENT MATERIALS 13
Thermomechanical Effects on Ir-W Alloys 13
Effect of Exposure to Oxygen and Carbon on the Physical and Mechanical Properties of Ir Alloys 13
Air Oxidation of Pt-3008 15
CURIUM-244 FUEL DEVELOPMENT 17
Compatibility Testing 17

IRIDIUM FABRICATION PROGRAM

A. C. Schaffhauser

Fabrication of Iridium for PICS

We are continuing production of Ir–0.3% W forming blanks for the post-impact containment shells (PICS) of the MHW Isotope Heat Source. Fabrication of blanks from recycled sheet scrap (WCR-series blanks) has been completed and 33 blanks were shipped. Characterization of microstructure, recrystallization, and chemical analysis showed that the recycled material is essentially the same as the original WC-series sheets.

Fabrication of blanks from the WE-series batch of powder is proceeding and 24 blanks were shipped. Initial recrystallization studies show that the recrystallization temperature for the WE-material is 100 to 150°C higher than for previous batches of powder. Development of a procedure for rolling 0.005-in. thick Ir–0.3% W for PICS weld shields and decontamination covers has also been completed. Foil has been shipped to MRC for forming evaluation. A summary of blanks shipped during the month is given in Table 1.

Cleaning Ir–0.3% W Sheet – (D. N. Braski)

Several changes and improvements have been incorporated in the cleaning procedure for Ir–0.3% W blanks. An electrolytic etching treatment is now performed on the blanks before they are acid cleaned and given their final stress-relieve anneal at 850°C. This additional step was added to remove tiny recrystallized grains on the blank surfaces that were apparently induced during the surface grinding process. It is desirable to remove these tiny grains to prevent the development of surface cracks during hydroforming at MRC. Chemical and Auger analyses are currently being conducted on KCN etched plus acid etched surfaces to determine if surface purity is further improved by the KCN electroetching procedure.

Acid cleaning of Ir–0.3% W blanks is now more effectively carried out in a special cleaning room fabricated for this program. The room

Table 1. Disposition and Characteristics of Ir–0.3% W Blanks

Ingot Number	Number Manufactured	Rejections			Number Shipped	Average Hardness (DPH)	Tungsten Content (ppm)
		Ultrasonic	Penetrant	Surface			
WCR-80	4	0	1[a]	0	4	527	3800
WCR-85	3	0	0	0	3	509	2500
WCR-86	4	0	0	1[b]	4	509	2900
WCR-87	2	0	0	1[b]	2	509	4000
WCR-89	3	0	0	0	3	516	2500
WCR-90	3	0	0	0	3	517	2900
WCR-92	4	1[a]	0	0	4	509	4000
WCR-93	4	1[a]	0	3	1	485	3500
WCR-94	4	2	0	1	1	484	3000
WCR-95	4	1[a]	0	1[b]	4	490	3200
WCR-96	4	0	0	1[b]	4	493	2900
WE-1	3	0	0	0	3	474	3500
WE-2	3	0	0	0	3	491	3500
WE-3	3	1	0	0	2	491	3000
WE-4	1	0	0	1[b]	1	515	3400
WE-5	3	1[a]	0	0	3	516	3000
WE-6	4	1[a]	0	0	4	516	2700
WE-7	3	0	0	0	3	520	3500
WE-8	3	0	0	1	2	512	2500
WE-9	4	0	0	1	3	505	2800
	66	3, 5[a]	1[a]	6, 5[b]	57		

[a] Nonconformance

[b] Visual note; in specification.

contains an acid hood, a large hooded-sink, and ultrasonic cleaning facilities. Teflon carriers and tanks of the type used by the semiconductor industry provides for safer and more uniform cleaning of the blanks and test discs in the hot acid solutions. The new teflon carriers have also enabled us to reduce the time spent acid cleaning since as many as 17 blanks can be processed through at one time. Ultrasonic agitation has been added to both the precleaning steps before the KCN etch and the final rinsing steps after the acid cleaning.

Recrystallization of Ir–0.3% W Sheet – (D. N. Braski)

A metallographic study was recently initiated to provide recrystallization data for a number of different lots of Ir–0.3% W sheet. The data will: (1) serve as a guide and check on the in-process fabrication anneals, (2) help MRC to determine the time and temperature for the final recrystallization anneal of the hydroformed Ir–0.3% W spheres, and (3) provide information for the final annealing of 0.005 and 0.010-in. thick Ir–0.3% W sheet. The results of this work are shown in Fig. 1. Groups of samples were first annealed for 15 min at temperatures from 750 to 1100°C in air. The samples were subsequently mounted, polished, and etched to reveal the microstructure. The percent of recrystallization in each sample was taken from the visually estimated ratio of recrystallized to unrecrystallized grains over the entire polished area. With exception of the 0.005-in. thick sample, WC-46, and 0.010-in. thick sample, WD-9/10 (ref. 1), all of the samples were 0.030-in. thick. Samples WD-3, WCR-89, and WD-9/10 were fully recrystallized after 15 min at 1100°C. Extrapolation of the data from lower temperatures show that these samples could be annealed at 1050°C to 1060°C for the same length of time and still be fully recrystallized. Sample WC-61 recrystallized about 25°C lower than the WD- and WCR-series samples. The WC-46 sample was almost completely recrystallized about 15 min at 950°C, which might be expected from the highly worked thin-gage material. The most surprising result was that for WE-1. The material in this lot showed no signs of any recrystallization until 1100°C was reached. It is estimated that at least 15 min at 1200°C

[1]Double wide ingot consisting of two ingots electron-beam welded together.

ORNL-DWG 74-1480

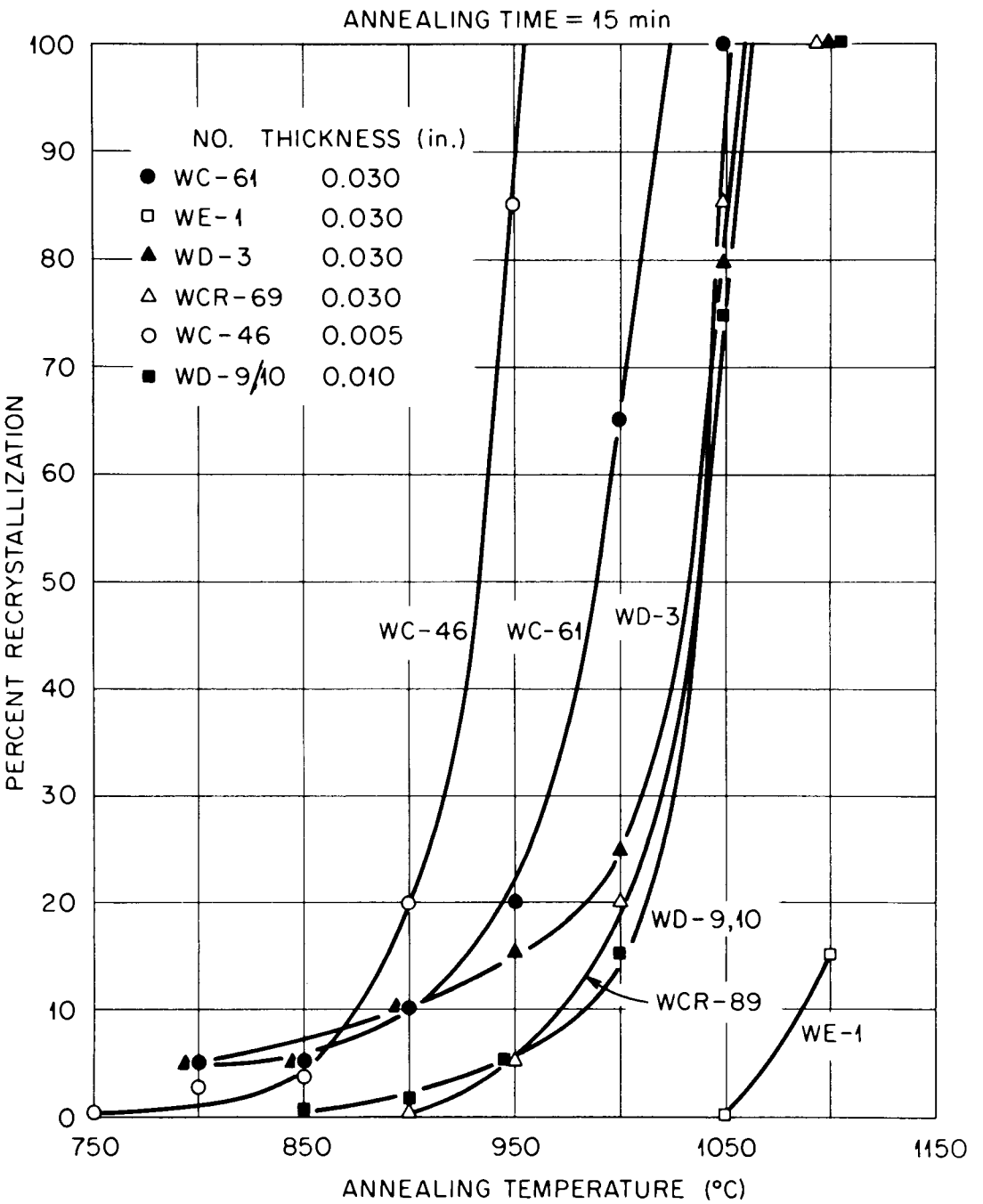

Fig. 1. Recrystallization Behavior of Various Ir–0.3% W Sheet Products Annealed for 15 min.

would be required to produce a fully recrystallized structure in the WE sheet. Appropriate changes in the annealing and rolling temperatures are being investigated. Additional samples are now being prepared to complete the data for WE-1 and a careful study of the chemistry for WE-lots is being conducted. Hardness values for all of the recrystallization samples are also being compiled.

Rolling 0.005-in. Thick Ir–0.3% W Sheet — (D. N. Braski and R. W. Knight)

We have completed development of a rolling procedure for fabrication of 0.005-in. thick Ir–0.3% W foil. The starting 0.032-in. thick sheet (approximately 10 1/2 in. × 3 in.) is first rolled bare at 950°C to produce a smooth surface finish. This condition is usually reached after bare rolling the sheet to a thickness of about 0.025 in. The sheet is further rolled between Inconel cover sheets (0.060-in. thick) at 800°C to a thickness of 0.015 in. After a one-hour anneal at 1000°C to recrystallize the sheet, it is further warm rolled at 800°C to the final 0.005-in. thickness. A high material yield (approximately 90%) having a good surface finish free of dye penetrant indications is produced using this process. The microstructure is uniformly fibrous and is free of delaminations.

HIGH-TEMPERATURE ALLOYS FOR SPACE ISOTOPIC HEAT SOURCES

H. Inouye

Development of Iridium Alloys

C. T. Liu and H. Inouye

Tensile Properties

Tensile specimens with a gage section of 1/2 × 1/8 in. were blanked successfully from sheet stock of Ir—10 wt % Ru after annealing 30 min at 1150°C. The specimens were then recrystallized 1 hr at 1500°C and tested at various temperatures in vacuum. The results are presented in Table 2 together with those for other Ir-Ru alloys. The yield and tensile strengths increase with Ru content. The ductility of the alloys is not sensitive to Ru content. In fact, all the Ir-Ru alloys have good ductility at impact temperature (i.e., 1370°C).

Air Oxidation

A study of the air oxidation of Ir—0.65% Hf, Ir—10% Ru, and Ir—8% Re alloys has continued. The sheet specimens were oxidized in the furnace at an air flow rate of 100 liters/hr at 770, 870, and 1000°C. The oxidation at 1000°C was terminated after an exposure of 330 hr. At present, the oxidation runs at 770 and 870°C have logged 1000 hr. The results indicate that the oxidation rate of Ir—8% Re is much higher than the other two alloys.

Scaleup of Iridium-Base Alloys

C. T. Liu and H. Inouye

Three Ir—1.92% W and three Ir—1.98% Re alloy ingots (3/4 × 3/4 × 2 1/8 in.) prepared from electron-beam melting of sintered alloy powder compacts were jacketed in TZM frames and hot rolled to 0.032-in.-thick sheets under an argon-filled furnace. The sheet fabrication involves the following steps (each step requires resizing the TZM frame and wrapping

Table 2. Tensile Properties[a] of Ir-Ru Alloy Sheets[b]

Alloy (wt %)	Strength, ksi Yield	Strength, ksi Tensile	Elongation (%)	Toughness (in./lb/in.^{3})
		Room Temperature		
Ir–0.5 Ru	11.0	24.0	5.2	
Ir–1 Ru	13.5	34.0	7.0	
Ir–2 Ru	22.5	55.4	8.4	
Ir–10 Ru	28.5	52.2	7.4	
		760°C		
Ir–0.5 Ru	9.0	42.0	17.0	
Ir–1 Ru	15.4	47.0	23.0	
Ir–2 Ru	13.7	69.2	25.2	
Ir–10 Ru	24.1	63.0	17.5	
		1093°C		
Ir–0.5 Ru	8.0	33.5	50.3	
Ir–1 Ru	12.5	31.4	35.5	
Ir–2 Ru	10.8	46.7	33.8	
Ir–10 Ru	13.6	52.6	33.7	
		1370°C		
Ir–1 Ru	8.0	23.0	45.4	7,000
Ir–2 Ru	9.0	32.8	52.3	10,900
Ir–10 Ru	12.2	37.4	43.4	10,800

[a]Tested in vacuum at a crosshead speed of 0.05 to 0.2 in./min.
[b]Specimens annealed 1 hr at 1500°C prior to testing.

in a new molybdenum cover sheet): The first rolling schedule consists of four passes at 25% each at 1300°C – two longitudinal passes and two transverse passes. After this schedule, the Ir–1.92% W and Ir–1.98% Re ingots were recrystallized 1 hr at 1450 and 1300°C, respectively. The second rolling schedule requires five passes – two at 25% and three at 20%, all cross rolled at 1130°C. The alloy plates with dimensions of 3 1/4 in. width × 0.1 in. thick were heat treated 1 hr at 1300°C. The final schedule reduced the alloy plates to 0.032-in.-thick sheet at 1130-1100°C at 10% reduction per pass, with all passes in the longitudinal direction. The final sheets were flat, smooth, and free from surface or

edge cracks. Thus, there was no difficulty in fabricating these two iridium-base alloys.

Tensile specimens were blanked from the Ir–1.98% Re sheet (heat No. Ir-45) and recrystallized 1 hr at 1500°C, then tested at temperatures up to 1370°C in vacuum. The tensile results are presented in Table 3. Compared with the tensile properties of the Ir–1.98% Re alloy sheet (heat No. Ir-14 in Table 3) fabricated from 150-g (0.3 × 1 × 2 in.) ingot button, Ir-45 shows a lower yield but a higher tensile strength. The ductility of the two sheets is not much different.

Table 3. Tensile Properties[a] of Ir–1.98% Re Alloy Sheets[b]

Heat Number	Strength, ksi		Elongation (%)
	Yield	Tensile	
	Room Temperature		
Ir-14[c]	26.0	67.6	8.9
Ir-45[d]	26.1	71.0	11.2
	760°C		
Ir-14[c]	19.3	67.3	28.0
Ir-45[d]	14.2	74.9	32.1
	1093°C		
Ir-14[c]	20.0	42.7	51.1
Ir-45[d]	15.0	43.8	45.0
	1370°C		
Ir-14[c]	12.6	30.0	55.4
Ir-45[d]	12.0	31.3	52.8

[a]Tested in vacuum at a crosshead speed of 0.05 to 0.2 in./min.

[b]Specimens annealed 1 hr at 1500°C prior to testing.

[c]Regularly cast ingot button, 2 × 1 × 0.3 in.; starting material: Matthey-Bishop iridium powder.

[d]Drop-cast ingot 2 1/8 × 3/4 × 3/4 in.; starting material: purified iridium powder.

Postmortem of MHT-74

C. T. Liu and H. Inouye

The fuel sphere assembly MHT-74, whose PICS were produced using ORNL/MRC Ir–1.92% W material, was impacted at GE and shipped to ORNL for postmortem analysis on January 17, 1974. The components of the assembly, their history and impact conditions are given below.*

PICS	Fuel Simulant	Impact Condition
Material: Ir–1.92 wt % W	Material: ThO_2	Velocity: 295 fps
Dimensions: pole to pole; 1.595 in; equator, 1.601 in.; 45°, 1.595 in.	Density: 76%	Temperature: 2600°F
	Weight: 219.2 g	Facility: GE
Surfaces: Grit blasted with WC		
Weight: 57.5 g		
Heat Treatment: 1 hr at 1500°C in vacuum		

*Based on the information obtained from GE and Mound Laboratory.

The Ir–1.92% W PIC deformed by flattening of the impact surface. Its dimensions were: diameter – 1.715 to 1.608 in.; height – about 1.2 in. This gives a maximum hoop strain of 7.2% occurring at the periphery. The back of the PIC showed no indication of deformation or damage. An indentation in the form of half circle with a diameter of about 3/4 in. was clearly observed just above the impact surface. Its formation is believed to be due to a severe rebounding impact. Cracks and microcracks were observed in two zones. Numerous cracks (fingerprints) were formed on the impact surface along concentric rings with a maximum and minimum diameter of 1/2 and 7/8-in., respectively. The impact surface was bulged outward due to the rebounding impact, causing some fingerprints to open up and go through the PIC shell. A few microcracks were also observed on the weld zone, but all were concentrated in a region directly opposite to rebounding impact. Only two of them breached the shell. The shell was sectioned and is ready for detailed metallographic examination.

Ruthenium Characterization and Fabrication Development

H. Inouye

Four sintered ruthenium compacts each weighing about 40 g were electron-beam melted into two buttons of about 80 g having the approximate dimensions, 5/16 × 1 1/8 × 1 7/16. Each button lost about 8 g after melting three times. The buttons are scheduled to be rolled to sheet between molybdenum cover plates and frames.

Platinum-Rhodium-Tungsten Alloys

H. Inouye

Fabrication Development

Studies of the ingot cracking problem during hot rolling and the causes for the ductility minimum in Pt-3008 (Pt-30% Rh-8% W) at about 1000–1100°C have continued. Ingot Pt-5D was electron-beam melted and drop-cast using scrap from prior heats that showed surface cracking during hot rolling. Surface cracks 0.005 to 0.010 in. deep again were present after hot rolling the ingot from 0.75 to 0.150 in. thick at 1200°C. Additional edge cracking occurred on rolling the conditioned plate to 0.040 in. thick at 1000°C and no further cracking occurred on cold-rolling to 0.020 in. thick sheet. Based on the studies to date, it is observed that (1) the severity of the surface cracks diminish each time the melting charge is remelted, and (2) the deleterious impurities are not effectively removed by electron-beam melting and are therefore not highly volatile. One suspected impurity is boron whose concentration, based on the analysis of the melting stock, is calculated to be about 50 ppm. Ingot Pt-5E was also electron-beam melted and drop-cast using scrap from normal ingots. Predictably, this ingot was rolled to 0.20 in. thick without any evidence of cracking. Tensile tests of both heats are scheduled next month.

Chemical analyses of tensile specimens showing a ductility range from 5 to 31% elongation at 1093°C revealed oxygen contents from <1 to 40 ppm. There was no correlation between ductility and oxygen content indicating that the ductility minimum is not related to the oxygen content of Pt-Rh-W

alloys. Auger, SSMS, and SEM analyses of selected specimens are in progress.

Fabrication of Compatibility Components

A replacement heat of Pt-3008 (heat Pt-5C) was rolled to 0.20 in. sheet from which 30 tensile specimens have been prepared for the Curium Program. A check of the tensile properties indicates that this heat has the expected tensile properties between room temperature and 1316°C. Final heat treatment of the tensile specimens will be done when fabrication of the fuel capsules has been completed.

PHYSICAL AND MECHANICAL METALLURGY OF HEAT-SOURCE CONTAINMENT MATERIALS

H. Inouye

Thermomechanical Effects on Ir-W Alloys

C. T. Liu

Tensile tests were performed to determine the mechanical properties of iridium and Ir-W sheets produced from iridium fabrication program. Tensile specimens were blanked from WD-1 (Ir-0.3W) and EBP-21 (Ir) sheet stocks and recrystallized 1 hr at 1500°C, then tested at temperatures up to 1370°C in vacuum. The tensile results are presented in Table 4 together with those for WC-4 (Ir-0.3W) and EI-114-C (produced at Engelhard Industries). Alloying with 0.3% W (WD-1 and WC-4) appears to strengthen the pure Ir(EBP-21). However, the sheet produced at Engelhard (EI-114-C) is the strongest among the four sheets. All the sheets have the same level of ductility at each temperature.

Effect of Exposure to Oxygen and Carbon on the Physical and Mechanical Properties of Ir Alloys

C. T. Liu

To characterize the compatibility between iridium-base alloys and the simulated heat-source environment, tensile sheet specimens of Ir-3.96% Re contacted with ATJ graphite on one side, were exposed to an oxygen pressure of 1×10^{-5} torr at 1300°C. Both sides of the specimens were bright and showed no indication of reaction with graphite and oxygen after a 1000-hr exposure. Weight measurement before and after the exposure showed an average loss of 43 ppm. The results of tensile tests of the exposed specimens are presented in Table 5 together with those for unexposed specimens. The data indicated that exposure to oxygen and graphite at 1300°C did not cause significant change in strength and ductility of the alloy. Thus, we conclude that Ir-3.96% Re is inert to the "simulated heat source environment" at 1300°C.

Table 4. Tensile Properties[a] of Ir and Ir-W Alloy Sheets[b]

Alloy (wt %)	Strength (ksi) Yield	Tensile	Elongation (%)
	Room temperature		
Ir (EBP-21)[c]	7.2	48.0	14.1
Ir–0.3 W (WC-4)[c]	13.4	55.7	12.1
Ir–0.3 W (WD-1)[c]	13.0	61.3	14.2
Ir (EI-114-C)[d]	13.3	63.2	13.5
	760°C		
Ir (EBP-21)[c]	8.2	56.9	38.4
Ir–0.3 W (WC-4)[c]	7.5	58.1	32.5
Ir–0.3 W (WD-1)[c]	9.3	58.7	42.5
Ir (EI-114-C)[d]	15.4	64.0	38.6
	1093°C		
Ir (EBP-21)[c]	8.5	37.0	50.6
Ir–0.3 W (WC-4)[c]	7.3	35.0	53.5
Ir–0.3 W (WD-1)[c]	10.6	36.8	55.3
Ir (EI-114-C)[d]	10.5	39.0	56.0
	1370°C		
Ir (EBP-21)[c]	7.4	23.0	50.4
Ir–0.3 W (WC-4)[c]	5.2	24.4	50.4
Ir–0.3 W (WD-1)[c]	7.8	23.8	56.0
Ir (EI-114-C)[d]	10.3	26.4	54.0

[a]Tested at a crosshead speed of 0.05 to 0.2 in./min in vacuum.

[b]Sheet specimens annealed 1 hr at 1500°C prior to test.

[c]Sheets produced at ORNL.

[d]Sheets produced at EI.

Table 5. Tensile Properties of Ir-3.96% Re Alloy Sheet Specimens Contacted with ATJ Graphite on One Side and Exposed to Oxygen at 1×10^{-5} torr at 1300°C

Exposure Time (hr)	Strength, ksi		Elongation (%)
	Yield	Tensile	
	Room Temperature		
0	32.1	60.6	6.4
1000	31.7	66.5	7.8
	760°C		
0	23.1	70.2	20.2
1000	17.0	78.8	25.1
	1370°C		
0	13.5	36.8	45.2
1000	12.3	34.8	34.5

Air Oxidation of Pt-3008

H. Inouye

The long term oxidation tests of Pt-3008 (heat Pt-4V) have logged 785.8 hr at temperatures of 600, 800, and 1000°C. Table 6 lists the average oxidation rates for two exposure times. The specimens at 600°C lose weight and those at 800 and 1000°C gain weight. A dark oxide film is present on specimens exposed at 800°C but no films are apparent at 600 or 1000°C.

Table 6. Air Oxidation of Pt-3008 (Pt-30% Rh-8% W) in Still Air[a]

Test Temperature (°C)	Exposure (hr)	Average Oxidation Rate[b] ($g\ cm^{-2}\ hr^{-1}$)	Weight Change (g/cm^2)
600	283.4	-4.9×10^{-8}	-1.4×10^{-5}
	785.8	-2.4×10^{-8}	-1.9×10^{-5}
800	283.4	$+3.3 \times 10^{-7}$	$+9.4 \times 10^{-5}$
	785.8	$+1.7 \times 10^{-7}$	$+1.3 \times 10^{-4}$
1000	283.4	$+1.8 \times 10^{-7}$	$+5.2 \times 10^{-5}$
	785.8	$+5.6 \times 10^{-7}$	$+3.9 \times 10^{-4}$

[a]Specimen dimensions: 0.020 × 0.62 × 1.0 in.

[b]Average for three specimens.

CURIUM-244 FUEL DEVELOPMENT

Compatibility Testing

J. R. DiStefano

Tests of $^{244}Cm_2O_3$ for 500 hr at 900 and 1400°C under the conditions outlined in Table 7 have been completed. They have been transferred to the High Radiation Level Examination Laboratory (HRLEL) where they will be opened and examined. It is expected that work will begin on these samples sometime in February.

Table 7. $^{244}Cm_2O_3$ Compatibility Test Materials for 500-hr Exposures at 900 and 1400°C

Set Number	Atmosphere	Test Materials and Conditions
		900°C
1	Helium	Ir, C, Pt, Hf–1% Pt–0.5% Pd, Hastelloy C-276, Haynes 25, Haynes 188, ThO_2, Pt–20% Rh, and Pt–26% Rh–8% W
2	Helium with graphite	Ir, Pt, Hf–1% Pt–0.5% Pd, Hastelloy C-276, Haynes 25, Haynes 188, ThO_2, Pt–20% Rh, and Pt–26% Rh–8% W
		1400°C
7	Helium with graphite	Ir, C, Mo, Mo–46% Re, Ta, T-111, W, and W–26% Re
8	Dynamic vacuum	Ir, Mo, Mo–46% Re, Ta, T-111, W, and W–26% Re
9	Helium	Ir, Mo, Mo–46% Re, Ta, T-111, W, and W–26% Re
10	Dynamic vacuum with graphite	Ir, C, Mo, Mo–46% Re, Ta, T-111, W, and W–26% Re

Control tests for the $^{244}Cm_2O_3$ compatibility tests referred to above were also completed and preliminary results (visual and weight change) are given in Tables 8 to 11. Some conclusions are drawn: (1) The precious metals were unaffected by exposure to helium, vacuum or graphite under the test conditions; (2) the superalloys reacted with graphite at 900°C but did not bond to the graphite when in contact; (3) molybdenum and tantalum reacted with graphite at 1400°C when there was surface contact; reaction was worse with molybdenum and with dynamic vacuum atmosphere compared with static helium.

Procurement of materials for the 16-couple test matrix is proceeding. Material and labor to produce finished test systems of Haynes-188, Ta—10% W, TZM, and W-26% Re are being provided by the Metals Division of Thermo Electron Company.

The alloy Mo-46% Re was available as sheet and plate from local stock. Pt-3008 alloy was first prepared by arc melting. It was then formed into sheet or rod by rolling or swaging, respectively. Capsules of both Mo-46% Re and Pt-3008 are being made from sheet using either standard or developmental forming techniques.

We received no reasonable bids from commercial vendors to make the ZrO_2 test system. Therefore, the design was modified so that commercially available ZrO_2 inserts fit inside a graphite container capsule. A rigidized ZrO_2 felt test specimen will be in contact with $^{244}Cm_2O_3$ and the ZrO_2 insert material, but not with graphite.

Three disk specimens of Si_3N_4 were received from N. Elsner of Gulf Energy and Environmental Systems. These specimens do not have satisfactory surface finishes and additional polishing will be required. Elsner reported that capsules of Si_3N_4 were unavailable and suggested we use molybdenum instead because it has good compatibility with Si_3N_4. A final decision has not yet been made.

Table 8. Summary of Preliminary Results on Control Tests[a] for Set No. 1 $^{244}Cm_2O_3$ Compatibility Tests

Material	Visual Observations		Weight Change (g)
	Capsule	Specimen	
Hastelloy C-276	Gray-black-gold film on outer surface, especially on end touching Al_2O_3	Dull	0
Haynes-188	Same as above, except gold film on top end not touching Al_2O_3	Dull	0
Haynes-25	Same as Hastelloy C-276	Dull	0
Hafnalloy-105	Dull, alumina-colored layer on outside surface, gold-colored layer below	Dull, black on surface touching capsule bottom	−0.0021
Graphite	No change on outside, but metallic layer on inside	Metallic layer on all surfaces except bottom where in contact with graphite capsule	0
Pt-20% Rh	Slightly dull appearance on outside	Bright, except bottom surface touching capsule	0
Pt-2608	Same as above	Bright	0

[a]900°C; 5000 hr; static helium; Al_2O_3 capsule holder; Hastelloy X outer container.

Table 9. Summary of Preliminary Results on Control Tests[a] for Set No. 2 $^{244}Cm_2O_3$ Compatibility Tests

Material	Visual Observations		Weight Change (g)
	Capsule	Specimen	
Hastelloy C-276	Gray-black layer on outer surface	Black	+0.0008
Haynes-188	Same as above	Black	+0.0006
Haynes-25	Light-gray layer on outer surface	Black	+0.0007
Hafnalloy-105	Gray-gold layer on outer surface	Dull, very light gold layer in some areas	0
ThO_2	Surface spotted gray-black-white	Same as capsule	0
Pt	Etched appearance	Bright, but etched appearance	0
Pt-20% Rh	Bright	Dull	0
Pt-2608	Bright	Bright, one dark spot	0
Ir	Bright	Bright	0

[a]900°C; 5000 hr; static helium; graphite intermediate capsule; graphite capsule holder; Hastelloy X outer container.

Table 10. Summary of Preliminary Results on Control Tests[a] for Set No. 7 $^{244}Cm_2O_3$ Compatibility Tests

Material	Visual Observations		Weight Change (g)
	Capsule	Specimen	
Mo	Bonded to graphite intermediate capsule, could not be separated	Etched but bright appearance	0
Ta	Dull on outer surface	Bright, large grains visible	0
T-111	Dull on outer surface	Dull	0
W	Shiny	Bright	Not obtained[b]
W-26% Re	Shiny	Dull to shiny	Not obtained[b]
Ir	Shiny, etched	Bright, etched	Not obtained[b]
Graphite	Light gray	No change	0

[a]1400°C; 5000 hr; static helium; graphite intermediate capsule; graphite capsule holder; Ta outer container.

[b]Specimen damaged when capsule was opened.

Table 11. Summary of Preliminary Results on Control Tests[a] for Set No. 10 $^{244}Cm_2O_3$ Compatibility Tests

Material	Visual Observations		Weight Change (g)
	Capsule	Specimen	
Mo	Bonded to graphite intermediate capsule. Inside surface irregular. Graphite appeared to have penetrated to inside. Capsule broken when we attempted to remove specimen - cleavage type fracture	Could not be removed. Reacted with graphite and capsule	Not obtained[a]
Mo-46% Re	Bonded to graphite; could not be removed	Bright	+0.0014
Ta	Bonded to graphite; could not be removed	Bright	0
T-111	Shiny	Shiny	0
W	Bright	Bright	Not obtained[b]
W-26% Re	Dull to shiny	Shiny	0
Ir	Bright, etched	Stuck to capsule; could not be removed. Shiny	Not obtained[b]
Graphite	Unchanged	Unchanged	0

[a]1400°C; 5000 hr; dynamic vacuum; graphite intermediate capsule; graphite capsule holder; Ta outer container.

[b]Specimen damaged when capsule was opened.

INTERNAL DISTRIBUTION

1. D. N. Braski
2. J. E. Cunningham
3. J. H. DeVan
4. J. R. DiStefano
5-9. R. G. Donnelly
10. J. I. Federer
11. M. R. Hill
12. H. Inouye
13. R. W. Knight
14. E. Lamb
15. C. T. Liu
16. C. L. Ottinger
17. R. E. McDonald
18. A. J. Moorhead
19. P. Patriarca
20. H. Postma
21. M. E. Ramsey
22. A. C. Schaffhauser
23. D. B. Trauger
24. T. N. Washburn
25. J. R. Weir, Jr.
26-27. Central Research Library
28. Document Reference Section
29-31. Laboratory Records
32. Laboratory Records, ORNL-RC
33. ORNL Patent Office

EXTERNAL DISTRIBUTION

34. M. Ault, Lewis Research Center
35-36. R. D. Baker, Los Alamos Scientific Laboratory
37. R. Brouns, Langley Research Center, NASA
38. R. T. Carpenter, Division of Space Nuclear Systems, AEC
39. W. T. Cave, Monsanto Research Corporation
40. G. R. Crane, Andrews AFB
41. G. Deutsch, NASA Headquarters
42. G. P. Dix, Division of Space Nuclear Systems, AEC
43. R. DuVal, San Francisco Operations Office
44. N. Elsner, Gulf Energy and Environmental Systems
45. J. Epstein, Goddard Space Flight Center, NASA
46. R. Fischell, Johns Hopkins University
47. D. S. Gabriel, Division of Space Nuclear Systems, AEC
48. N. Goldenberg, Division of Space Nuclear Systems, AEC
49. E. F. Hampl, Minnesota Mining and Manufacturing Company
50. W. S. Hollman, Division of Applied Technology, AEC
51. R. G. Ivanoff, Jet Propulsion Laboratory
52. H. Jaffe, Division of Space Nuclear Systems, AEC
53. E. W. Johnson, Monsanto Research Corporation
54. G. W. Johnson, Division of Applied Technology, AEC
55. I. Jones, TRW Systems
56. R. J. Katucki, General Electric Company
57. D. P. Kelly, Monsanto Research Corporation
58. T. B. Kerr, NASA Headquarters
59. J. Linkous, Isotopes, Inc.
60. J. J. Lombardo, Division of Space Nuclear Systems, AEC
61. J. N. Maddox, Division of Biomedical and Environmental Research, AEC
62. J. McDonald, Sandia Laboratories
63. R. N. R. Mulford, Los Alamos Scientific Laboratory

64. H. Nelson, Ames Research Center, NASA
65. T. A. Nemzek, Division of Reactor Research and Development, AEC
66. G. A. Newby, Division of Space Nuclear Systems, AEC
67. A Noonan, Kirtland AFB
68. D. Ofte, Albuquerque Area Office, AEC
69. W. Pardue, Battelle Memorial Institute
70. T. E. Redding, Manned Spacecraft Center
71. R. W. Shivers, Division of Applied Technology, AEC
72. J. M. Simmons, Division of Reactor Research and Development, AEC
73. A. A. Solomon, Argonne National Laboratory
74. M. D. Starr, Naval Facilities Engineering Command
75. C. O. Tarr, Division of Space Nuclear Systems, AEC
76. V. Truscello, Jet Propulsion Laboratory
77. D. R. Turno, Savannah River Laboratory
78. E. J. Wahlquist, Division of Space Nuclear Systems, AEC
79. R. L. Wainwright, Dayton Area Office, AEC
80. D. Watrous, Donald W. Douglas Laboratories
81. A. Wilbur, Ames Research Center, NASA
82. Directorate of Nuclear Safety, Kirtland AFB
83. Research and Technical Support Division, ORO
84-85. Technical Information Center, OR